

Comparative studies of the structural and electrical studies of conventional and microwave sintered $\text{Li}_{0.35}\text{Ni}_{0.1}\text{Mn}_{0.1}\text{Zn}_{0.2}\text{Fe}_{2.35}\text{O}_4$ synthesized by the citrate precursor method

Sanatombi Sorokhaibam^{1*}, Ibetombi Soibam¹, Sumitra Phanjoubam²

¹Department of Physics, National Institute of Technology, Manipur, Langol 795004, India

²Manipur University, Canchipur, Imphal 795003, India

*Corresponding author, Email: sanatombis1@gmail.com

Received: 28 March 2016, Revised: 27 September 2016 and Accepted: 30 November 2016

DOI: 10.5185/amp.2017/115

www.vbripress.com/amp

Abstract

Substituted lithium ferrite having the chemical formula $\text{Li}_{0.35}\text{Ni}_{0.1}\text{Mn}_{0.1}\text{Zn}_{0.2}\text{Fe}_{2.35}\text{O}_4$ have been synthesized by the citrate precursor method. The sample was given pre-sintering at 650°C in a conventional furnace. Final sintering was carried out at 900°C in a conventional surface and another in a microwave furnace. The spinel phase structure of the conventional (CS) and microwave sintered (MS) samples was confirmed by the XRD patterns. From the analysis of XRD data, the crystallite size of the samples was estimated and smaller crystallite size was observed in the microwave sintered sample. Scanning Electron Microscopy (SEM) was also carried out. The dielectric studies were investigated. Room temperature dielectric constant (ϵ') and dielectric loss ($\tan \delta$) were studied as a function of frequency. Experimental results show dispersion for variation of dielectric constant and dielectric loss tangent with frequency for both CS and MS sample. However, microwave sintered sample show lower dielectric constant and losses. Possible mechanism is being discussed. Copyright © 2016 VBRI Press.

Keywords: Ferrite, conventional sintering, microwave sintering, dielectric constant, dielectric loss, polarization.

Introduction

Spinel ferrite is one of the important ferrimagnetic materials having the chemical formula MFe_2O_4 where M is the divalent ion. They have been found to be used in various technological applications ranging from microwave to radio frequencies [1-5]. A low dielectric constant and low dielectric loss etc. makes the material demanding for certain application. The dielectric properties can be tailored by the synthesis method, substitution and sintering technique [6-9]. As far as synthesis method is concern, low temperature synthesis technique is preferred to avoid the volatilization of lithium and oxygen ion. There are several methods to synthesize lithium and substituted lithium ferrites material such as solid state reaction, sol-gel, chemical co precipitation, citrate precursor etc. [10-16]. A very simple and economic method is citrate precursor method. Considering the substituent, there are various substituent ions such as Cu^{2+} , Cd^{2+} , Zn^{2+} , Mn^{2+} etc. as reported by several workers. However, addition of Ni ion reduces power loss which makes them useful for power application [3]. Besides these, addition of Ni and Zn ion in the basic lithium ferrite improved densification [16, 17]. Further the overall properties may also be affected by sintering technique

used. A technique which is microwave sintering in which heat is generated internally within the sample and taking less time instead of transferring thermal energy from external sources and took longer time which happens in a conventional sintering is becoming an area of investigations [18-21].

Therefore, in the present work, a comparative study of the structural and dielectric properties of Lithium Nickel Manganese Zinc ferrite sintered using the conventional and microwave sintering techniques is being discussed.

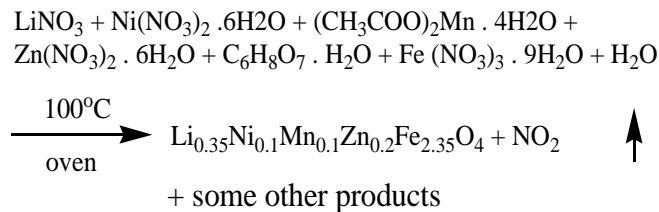
Experimental

Materials

The chemicals used were Lithium nitrate (LiNO_3 , purity-98%, Merck, Germany), Nickel (II) nitrate hexahydrates, ($\text{Ni}(\text{NO}_3)_2 \cdot 6\text{H}_2\text{O}$, purity-98%, Merck, India), Manganese (II) acetate tetra hydrates cryst. Pure ($\text{Mn}(\text{CH}_3\text{COO})_2 \cdot 4\text{H}_2\text{O}$, purity-99%, Merck, India), Zinc nitrate hexahydrate Purified, ($\text{Zn}(\text{NO}_3)_2 \cdot 10\text{H}_2\text{O}$, purity-96%, Merck India), Iron(III) nitrate nonahydrates Purified ($\text{Fe}(\text{NO}_3)_3 \cdot 9\text{H}_2\text{O}$, purity – 98%, Merck, India) and Citric acid ($\text{C}_6\text{H}_8\text{O}_7 \cdot \text{H}_2\text{O}$ purity-99%, Merck, India). In all the synthesis, distilled water (EMPLURA) is used as a solvent.

Material synthesis

Nickel substituted lithium ferrite with chemical formula $\text{Li}_{0.35}\text{Ni}_{0.1}\text{Mn}_{0.1}\text{Zn}_{0.2}\text{Fe}_{2.35}\text{O}_4$ was synthesized by the citrate precursor method. Stoichiometric amount of lithium nitrate, zinc nitrate, manganese acetate, iron nitrate and citric acid were mixed together for making a solution. Metal ion and citric acid are taken in the ratio of 1:1. The resulting solution was refluxed at 40°C till it appears transparent clear solution. Then ammonia solution is added drop by drop to maintain the pH value at 7 and stir continuously for half an hour. The pH controlled solution was then put in an oven at 100°C . Finally, auto combustion takes places giving the required ferrite material. The following chemical reaction takes place during combustion as



The final product so obtained is the typical spinel structured LNMZ powder with nano crystallite size. Polyvinyl alcohol was added as binder for the synthesized powder and pressed into pellets. It was then given pre-sintering at 600°C with a heating rate of $5^\circ\text{C}/\text{min}$ for 3hrs in a conventional furnace. The final sintering was carried out at 900°C for 3hrs at a heating rate of $5^\circ\text{C}/\text{min}$ by conventional sintering technique and at the same temperature for 30 minutes at a heating rate of $10^\circ\text{C}/\text{min}$ by microwave sintering technique.

Characterizations

Spinel phase structure of the CS and MS sample was identified by X Pert Pro X-Ray Diffractometer with scanning range from $20^\circ - 80^\circ$ using $\text{Cu-K}\alpha$ radiation of incident wavelength $\lambda=1.5405 \text{ \AA}$. From XRD data lattice parameter was calculated using the relation

$$a = d_{hkl}(h^2 + k^2 + l^2) \quad (1)$$

where, a is the lattice parameter, d is the interplanar spacing and h, k, l are miller indices.

The Crystallite size was calculated using Debye Scherrer's relation

$$D_{cryst} = \frac{0.89\lambda}{\beta \cos\theta} \quad (2)$$

Scanning Electron microscopy (SEM) micrograph of the fractured surface was recorded using Scanning Electron Microscope FEI Quanta 250. The dielectric studies such as dielectric constant and dielectric loss were carried out by using Agilent LCR Meter Precision E4980.

Results and discussion

Structural studies

Fig. 1. shows the X-ray diffraction patterns of the synthesized sample confirmed the formation of single phase spinel structure of the synthesized sample. The observation patterns show diffraction peaks corresponding to the lattice planes of (220), (311), (400), (422) (333), (440) etc. All the peaks could be indexed to the standard pattern reported by the Joint Committee on Powder Diffraction Standards (JCPDS card no. 88-0671). No extra peak is found indicating that no impurities are present. The estimated value of the lattice parameter and crystallite size calculated from the analysis of XRD data are $0.829 \text{ nm}(\text{CS})$ and $0.830 \text{ nm}(\text{MS})$ and $65 \text{ nm}(\text{CS})$, $59 \text{ nm}(\text{MS})$ respectively.

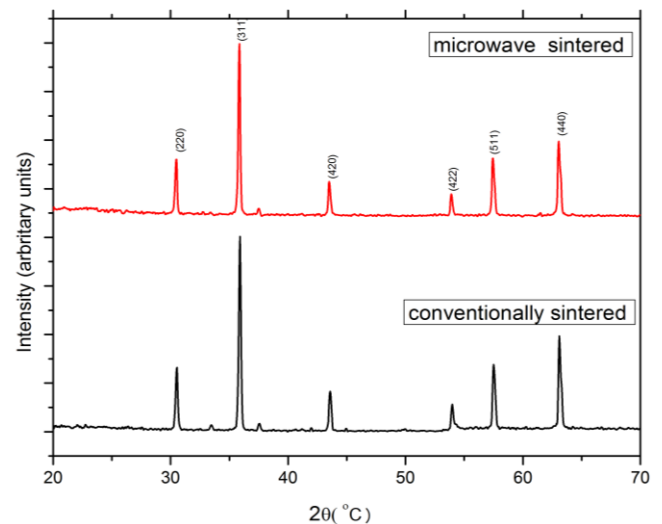


Fig. 1. XRD patterns of the CS and MS $\text{Li}_{0.35}\text{Ni}_{0.1}\text{Mn}_{0.1}\text{Zn}_{0.2}\text{Fe}_{2.35}\text{O}_4$ samples.

The photo micrograph images of the CS and MS samples is shown in Fig. 2 and it was observed that MS samples show smaller grain size distribution compared to CS sintered sample. Several workers reported that MS sample show larger grain size compared to CS sample which was explained on the basis of the dependence of several transport phenomena, permittivity etc. In our case the observed lower value may be due the fact that the sintering is still in the initial stage. [6, 7, 21].

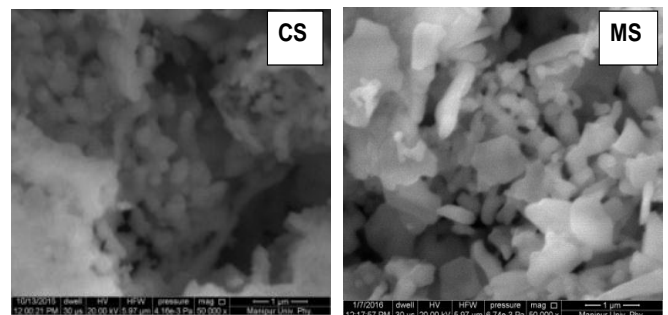


Fig. 2. SEM micrograph of the CS and MS $\text{Li}_{0.35}\text{Ni}_{0.1}\text{Mn}_{0.1}\text{Zn}_{0.2}\text{Fe}_{2.35}\text{O}_4$ sample.

Dielectric studies

Fig. 3(a) shows the variation of dielectric constant with frequency of the applied field for conventionally and microwave sintered LNMZ ferrite.

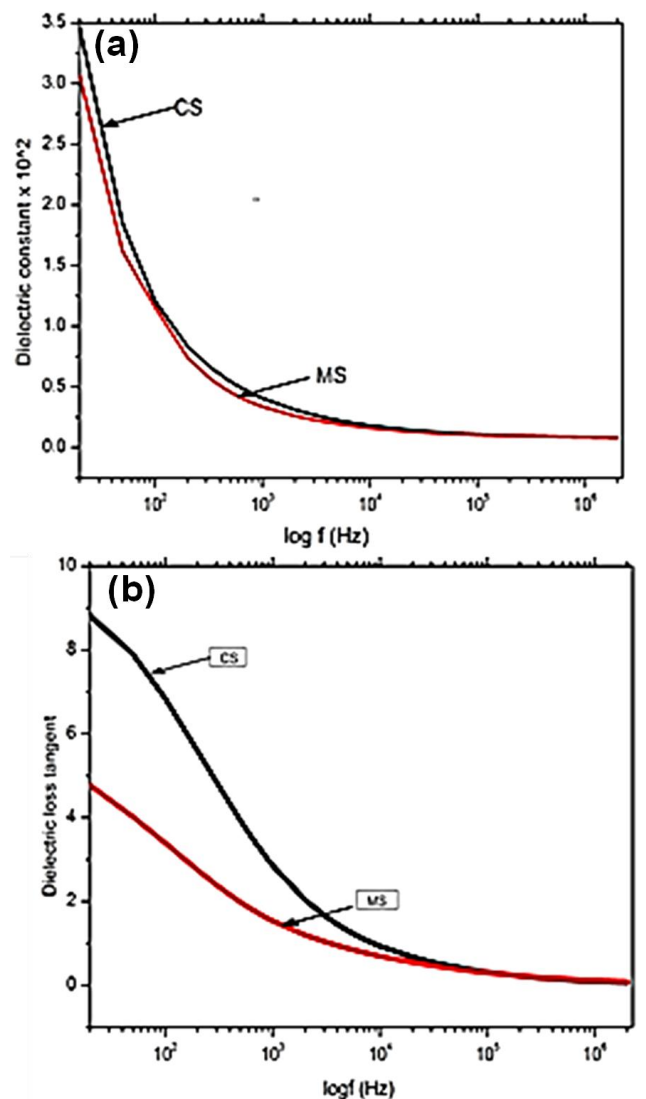


Fig. 3. (a) Variation of dielectric constant with frequency for CS and MS LNMZ ferrite sample. (b) Variation of dielectric loss tangent with frequency for CS and MS LNMZ ferrite sample.

The observed dispersion in variation of dielectric constant with frequency for CS and MS sample can be explained in term of space charge polarization and Koop's two-layer model [22, 23]. According to the model, ferrite is assumed to be made up of well conducting grains separated by poor conducting grain boundaries. The electrical conduction in ferrite is explained by Verwey mechanism in terms of the hopping of electrons between Fe^{2+} and Fe^{3+} ions at B sites. The electrons reach the grain boundary by hopping and pile up due to its poor conductivity. This produces the space charge polarization. In the present study, at low frequency of the applied field, the grain boundary having poor conductivity hinders the hopping motion of electrons creating space charge

polarization, leading to a high dielectric constant. As the frequency of the applied field increased, the resistivity of grain boundary decreases and the electronic exchange is not able to follow the alternating field and the electron reverse the direction of motion thereby decreasing the probability of electron reaching the grain boundary. Consequently, the dielectric constant decreases. At still higher frequency, the probability of creating space charge polarization is small and become almost independent of frequency. MS samples show lower dielectric constant compared to conventional sintered sample. This may be due to the less formation of Fe^{2+} ion because of less heating time and rapid heating rate [7, 25]. However, a detail investigation is required.

Fig. 3(b) shows the variation of room temperature dielectric loss tangent with the frequency for conventional and microwave sintered samples.

Both shows dispersion which was the normal behavior of ferrite as was reported earlier by others workers [6, 14, 21, 24]. However, MS sample show lower loss value as compared to CS sample [7, 25]. This may be attributed to the low loss of energy and the samples take short processing time thereby saving the expenditure of energy.

Conclusion

Lithium Nickel Manganese zinc ferrite was successfully synthesized by the citrate precursor method. Experimental results indicate that the microwave sintered sample show lower particle size, low dielectric constant and low dielectric losses as compared to conventionally sintered samples. Less heating time and rapid heating rate may be responsible for the formation of less Fe^{2+} ion in MS samples decreasing the value of dielectric constant. However, a detail investigation is needed so as to make possible application

Acknowledgements

Authors would like to thank Manipur University for XRD and SEM measurement.

Author's contributions

Synthesis, characterization, data collection, analysis were done by Sanatombi S, The research paper was written by Sanatombi S, Ibteombi S and Sumitra P.

References

- Horvath, M. P.; *J. Magn. Magn. Mater.*, **2000**, 215, 171. DOI: [10.1016/S0304-8853\(00\)00106-2](https://doi.org/10.1016/S0304-8853(00)00106-2).
- Sun, C.; Sun, K.; *Solid state Commun.*, **2007**, 141, 258. DOI: [10.1016/j.ssc.2006.10.039](https://doi.org/10.1016/j.ssc.2006.10.039)
- Kotnala, R. K.; Dar, M. M.; Verma, V.; Singh, A. P.; Siddiqui, W.A.; *J. Magn. Magn. Mater.*, **2010**, 322, 3714. DOI: [10.1016/j.jmmm.2010.07033](https://doi.org/10.1016/j.jmmm.2010.07033)
- Singh, V.; Tiwari, A.; *Carbohydrate research*, 2008, 343, 151.
- Soibam, I.; Sorokhaibam, S.; *American Journal of Material Science and Engineering.*, **2014**, 2, 42. DOI: [10.1269/ajmse-2-3-3](https://doi.org/10.1269/ajmse-2-3-3)
- Shannigrahi, S.; Tannn, I.K.C.; *Technologies.*, **2015**, 3, 47. DOI: [10.3390/technologies3010047](https://doi.org/10.3390/technologies3010047)
- Raghupathi, C.; Vijaya, J. J.; Kennedy, J. L.; *J. Saudi Chem. Soc.*, **2014** DOI: [10.1016/j.jscs.2014.006](https://doi.org/10.1016/j.jscs.2014.006)

8. Soibam, I.; Phanjoubam, S.; Sharma, H.B.; Sarma, H.N.K.; Laishram, R.; Prakash, C; *Solid State Commun.*, **2008**, *148*, 399.
DOI: [10.1016/j.ssc.2008.09.029](https://doi.org/10.1016/j.ssc.2008.09.029)
9. Verma, V.; Pandey, V.; Singh, S.; Aloysius, R. P.; Annapoorni, S.; Kotanala, R. K; *Physica B.*, **2009**, *404*, 2309.
DOI: [10.1016/j.physb.2009.04.034](https://doi.org/10.1016/j.physb.2009.04.034)
10. Aruna, S. T.; Mukasyan, A. S; *Curr. Opin. Solid State Mater. Sci.*, **2008**, *12*, 44.
DOI: [10.1016/j.cossms.2008.12.002](https://doi.org/10.1016/j.cossms.2008.12.002)
11. Zaki, H. M.; Al-Heniti, S.; Umar, A.; Al-Marzouki, F.; Abdel-Daiem, A.; Elmosalami, T.A.; Dawoud, H.A.; Al-Hazmi, F.S.; Ata-Allah, S.S ; *J. Nanosci. Nanotechnol.*, **2013**, *13*, 4056.
DOI: [10.1166/jnn.2013.7434](https://doi.org/10.1166/jnn.2013.7434)
12. Hessian, M. M; *J. Magn. Magn. Mater.*, **2008**, *320*, 2800.
DOI: [10.1166/jnn.2008.06.018](https://doi.org/10.1166/jnn.2008.06.018)
13. Kadam, R. H.; Biradar, A. R.; Mane, M. L.; Shirsat, S. E; *J. Appl. Phys.*, **2012**, *112*, 043902.
DOI: [10.1063/1.4746746](https://doi.org/10.1063/1.4746746)
14. Maisnam, M.; Phanjoubam, S.; *Solid state commun.*, **2012**, *152*, 320.
DOI: [10.1016/j.ssc.2011.11.019](https://doi.org/10.1016/j.ssc.2011.11.019)
15. S.A Mazen and Elmosalami T.A; *Int. Sch. Res. Notices.*, **2011**, *9*, 820726.
DOI: [10.5402/2011/820726](https://doi.org/10.5402/2011/820726)
16. Verma, A.; Chatterjee, R; *J. Magn. Magn. Mater.*, **2006**, *306*, 313.
DOI: [10.1016/j.jmmm.2006.03.033](https://doi.org/10.1016/j.jmmm.2006.03.033)
17. Sattar, A.A.; El-Sayed, H.M.; Agami, W.R; *Am. J. Appl. Sci.*, **4**, 89.
DOI: [10.3844/ajassp.2007.89.93](https://doi.org/10.3844/ajassp.2007.89.93)
18. Sanakaranarayan V.K.; Sreekumar C.; *Curr. Appl. Phys.*, **2003**, *3*, 205.
DOI: [10.1016/S1567-1739\(02\)00202-X](https://doi.org/10.1016/S1567-1739(02)00202-X)
19. Brevall E.; Cheng J. P.; Agrawal D. K.; Gigl P.; Dennis M.; Roy R.; Papworth A.; *J. Mater. Sci. Eng., A.*, **2005**, *391*, 285.
DOI: [10.1016/j.msea.2004.08.085](https://doi.org/10.1016/j.msea.2004.08.085)
20. Penchal R. M.; Madhuri M.; Shadhana K.; Kim I.G.; Hui K.N.; Siva K.K.V.; Ramakrishna R. R ; *J. Sol-Gel Sci. Technol.*, **2014**, *70*, 400.
DOI: [10.1007/s10971-014-3295-7](https://doi.org/10.1007/s10971-014-3295-7)
21. Kuruva P.; Rajaputra, S. U. M. S.; Sanyadanam, S.; Sarabu M. R.; *Turk. J. Phys.*, **2013**, *37*, 312.
DOI: [10.3906/fiz-1303-4](https://doi.org/10.3906/fiz-1303-4)
22. Koops, C.G.; *Phys. Rev.*, **1951**, *1*, 121.
DOI: [10.1103/PhysRev.83.121](https://doi.org/10.1103/PhysRev.83.121)
23. Soibam, I.; Phanjoubam, S.; Radhapiyari, L.; *Physica B.*, **2010**, *405*, 2181.
DOI: [10.1016/J.Physb.2010.01.131](https://doi.org/10.1016/J.Physb.2010.01.131)
24. Shannigrahi Santiranjan; Tannn Ivaaan Kianngng Chee, *Technologies*, **2015**, *3*, 47.
DOI: [10.3390/technologies3010047](https://doi.org/10.3390/technologies3010047)
25. Kumar, P.; Juneja, J.K.; Prakash, C.; Singh, S.; Ravi, K.; Raina, K.K; *Ceram. Int.*, **2014**, *40*, 2501.
DOI: [10.1016/j.ceramint.2013.07.063](https://doi.org/10.1016/j.ceramint.2013.07.063)
26. Raman R; Murthy K.R.V; Vishwanathan; *J. Appl. Phys.*, **1991**, *7*, 69.
27. Yen - Pei Fu, Chin-Shang Hsu; *Solid State Commun.*, **2005**, *134*, 201.
DOI: [10.1016/j.ssc.2004.12.035](https://doi.org/10.1016/j.ssc.2004.12.035)
28. Hench L.L.; West, J.; Principles of electronic ceramics: John Wiley and sons
29. Rezlescu, N.; Doroftei, C.; Popa, P. D; *Sens. Actuators B Chem.*, **2008**, *133*, 420.
DOI: [10.1016/j.snb.2008.02.047](https://doi.org/10.1016/j.snb.2008.02.047)